Noise Suppression of Nd:YVO_4 Solid-State Lasers for Telecommunication Applications

Márk Csörnyei, *Student Member, IEEE*, Tibor Berceli, *Fellow, IEEE*, and Peter R. Herczfeld, *Fellow, IEEE*

***Abstract*—This paper is intended to elaborate on the investigation and suppression of the relative intensity noise of a diode pumped Nd:YVO_4 microchip laser. In addition to noise suppression at the relaxation oscillations, noise analysis is also reported. For these investigations a very simple, rate-equation-based model of the laser transfer function was used.**

***Index Terms*—Laser noise, neodymium:solid lasers, optical communication.**

I. Introduction

THERE is a comprehensive interest in laser diode pumped solid-state lasers like Nd:YVO_4. Owing to their high output power and excellent phase noise characteristics, they can be made use of on different fields, such as telecommunication and industrial applications.

The intensity noise of microchip lasers is a crucial parameter in many systems, like gravitational wave detection, rare-earth-doped fiber amplifiers, or optically fed mobile radio base stations. Therefore, significant effort is being expended to investigate and reduce the noise of these lasers.

In contrast to other crystal lasers, Nd:YVO_4 has proved to be a good choice because of its strong broadband absorption at 808 nm. Thus it is quite insusceptible to heating-caused wavelength instability of the pump laser diode. However, it also suffers from the intensity noise peak at the relaxation resonance. At the frequency of the relaxation oscillations the noise has a high peak, 30–40 dB higher than that outside the resonance region. This resonant range is between 100 kHz–2 MHz with a resonant frequency defined by the pump power.

There have been a number of publications recently on noise suppression and its possible application in fiber radio systems. Herczfeld [1] and Jemison *et al.* [2] examined the use of a Nd:$LiNbO_3$ mode-locked laser in a local multipoint distribution system (LMDS). Because of the good phase noise characteristics, the optical generation of the local oscillator signal is feasible. However, the suppression of the relaxation oscillations close to the carrier can improve the quality of the whole system. A number of feedback loops for different types of lasers have been evaluated and their corresponding advantages discussed. Kane [3] and Harb [4] have designed an electronic feedback for the reduction of intensity noise in a diode pumped Nd:YAG laser. Similarly, Geronimo [5] and Taccheo [6] investigated the intensity noise reduction in an ytterbium-codoped erbium glass laser. In addition, the noise suppression with an external feedback was studied by Ni [7].

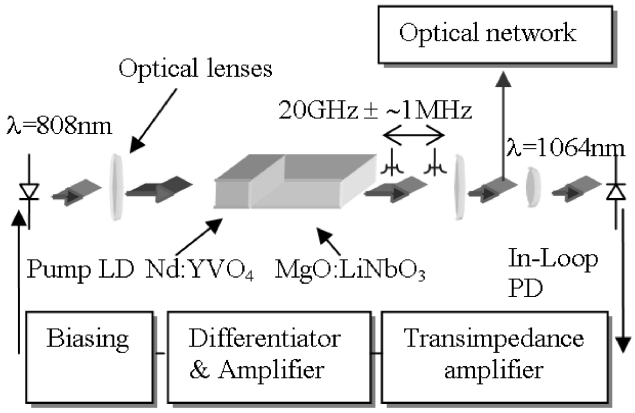

Fig. 1. Feedback loop for intensity noise suppression. The two modes of the laser are 20 GHz apart.

However, the references mentioned did not look into the dependence of the relaxation oscillation frequency on the output power of the pumping laser diode. Regarding our previous report [8], significant improvement was made by using Nd:YVO_4 instead of Nd:$LiNbO_3$ and changing the Si PIN to InGaAs photodiode in the feedback loop. These innovations made it possible to reduce the overall system noise and to carry out new investigations. This paper presents a realized approach to suppressing the relative intensity noise (RIN) peak by active feedbacking, considering the tune of the peak.

The structure of this paper is as follows. Section II presents the theory of the suppression, the computer simulations, and the calculation results. Section III outlines the optical subsystem and the noise characteristics. Sections IV and V exhibit the feedback loop electronics and the noise suppression. Section VI summarizes the results of this paper and the further possible efforts in this field.

II. Theory of the Suppression Loop

The block diagram of the feedback loop used for noise suppression is depicted in Fig. 1. A fraction of the laser output signal is detected, differentiated, phase shifted, amplified, and fed back to the pump laser dc supply. The output wavelength of the laser crystal is 1064 nm and needs a pump power at the

Manuscript received April 29, 2003; revised July 29, 2003. This work was supported in part by the National Research Foundation under OTKA T030148.

M. Csörnyei and T. Berceli are with the Department of Broadband Infocommunication Systems, Budapest University of Technology and Economics, H-1111 Budapest, Hungary (e-mail: mark.csornyei@mht.bme.hu; berceli@mht.bme.hu).

P. R. Herczfeld is with the Center for Microwave-Lightwave Engineering, Drexel University, Philadelphia, PA 19104 USA (e-mail: pherczfe@cbis.ece.drexel.edu).

Digital Object Identifier 10.1109/JLT.2003.821735

TABLE I
PARAMETERS OF 1.1% DOPED ND:YVO_4. ATTENUATION, THRESHOLD POWER, EMISSION CROSS-SECTION, PHOTON DECAY TIME, AND THE CALCULATED POWER DENSITY CONSIDERING THE CROSS-SECTION AREA (0.6 × 3 mm) OF THE CRYSTAL

α (1/cm)	P_{th} (mW)	σ (cm^2)	τ_c (s)	I (W/cm^2)
9.2	78	$7*10^{-19}$	$3.623*10^{-12}$	4.33

wavelength of 808 nm. Prior to designing the feedback loop, rate-equation-based calculations and modeling of the relaxation oscillations were carried out. In order to be able to model the impulse response and the transfer function of the Nd:YVO_4 crystal laser, we had to evaluate the corresponding rate equations [9]. As an input for the impulse response calculations, small perturbations of the population inversion Δn and the photon density $\Delta\phi$ had to be introduced. Eliminating the population inversion, we can evaluate the following solution for the photon density impulse response [9] (1):

$$\Delta\phi \approx \exp\left(-\frac{\sigma c\phi}{2}\right) t \sin\left[\sigma c(\phi n)^{1/2}\, t\right] \tag{1}$$

where σ is the emissions cross-section, n is the electron population density, and ϕ is the photon density. Based on (1), the frequency of the oscillation can be expressed by the intercavity power density $I = c\phi h\nu$ and the photon decay time τ_c [9]. The frequency of the relaxation oscillations is represented in (2)

$$\omega = \sqrt{\frac{\sigma I}{\tau_c h\nu}}. \tag{2}$$

The necessary parameters of Nd:YVO_4 are shown in Table I.

Substituting these parameters into (2), we have a value for the relaxation oscillation frequency of 336 kHz. This frequency was calculated at a minimum threshold power of 78 mW.

Equation (1) allows us to use a very simple transfer function of (3) for the modeling of the laser relaxation oscillation characteristics. This function has a similar impulse response, as shown in (1)

$$G(s) = \frac{1}{1 + 2dTs + T^2 s^2}. \tag{3}$$

In the modeled transfer function of $G(s)$, d defines the value of the complex conjugate poles and consequently the height of the noise peak, and T gives the frequency of the resonance. The Bode plot of the modeled transfer function is shown in Fig. 2. According to the measured results (Figs. 5 and 6), there is a high peak and almost 180° phase shift at the relaxation resonance. The RIN model has the transfer function $G(s)$; therefore the transfer function of the closed loop is shown in (4), where $\beta(s)$ is the transfer function of the feedback system

$$F(s) = \frac{G(s)}{1 + G(s)\beta(s)}. \tag{4}$$

If the optical and electrical delay is taken into account, the above expression should be changed to the formula of (5)

$$F(s) = \frac{G(s)}{1 + G(s)\beta(s)e^{-s\tau}}. \tag{5}$$

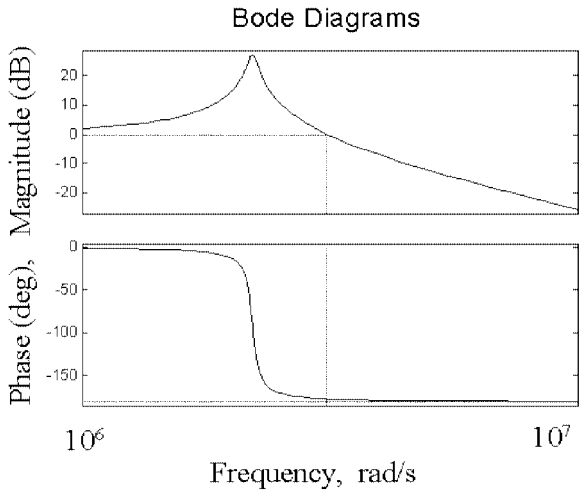

Fig. 2. Bode plot of the simulated crystal transfer function. There is a 30-dB resonance at the relaxation oscillation, which is caused by the complex conjugate poles. Since the phase diagram shows only a very small phase margin at the oscillation frequency, special attention had to be given while designing the control loop.

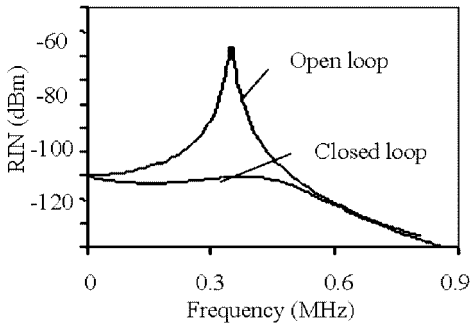

Fig. 3. RIN suppression simulation at the relaxation oscillation frequency.

The time delay could cause instability in the system, so it should be kept as low as possible.

The noise peak in the 100 kHz–2 MHz range of the optical carrier is to be reduced by using negative feedback. As the transfer function of the laser transmitter has a phase shift of almost $-180°$ near the frequency where the gain of the open loop goes below unity, we have to realize positive phase shift in the amplifier following the low-noise photodiode.

To neutralize the complex conjugate poles of the crystal transfer function, we have to use a differentiator circuit with a zero near the relaxation oscillation frequency. The zero of the differentiator in the feedback circuit can compensate the effect of the complex conjugate poles of the microchip laser transfer function, which are responsible for the high noise peak. There is also an additional pole of the differentiator at a higher frequency (10 MHz), which is only necessary because of the stability of the differentiator circuit and does not have any influence in the frequency range of the peak. As is shown in Fig. 1, the differentiator circuit is followed by an amplifier and the laser diode bias circuit.

The results of the computer simulations are depicted in Fig. 3. The real disturbing resonance term (open loop) stands out by 50 dB from the outside region.

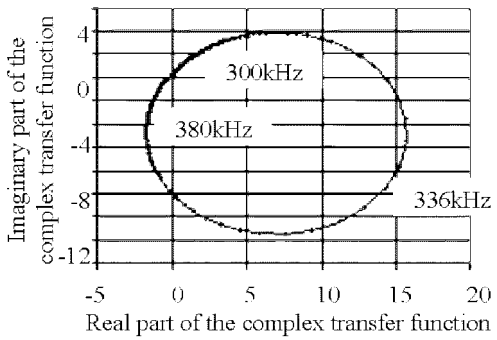

Fig. 4. The Nyquist diagram of the control loop. The maximum is at 336 kHz in the positive–negative quadrant of the diagram. The instability point is not encompassed by the curve; hence the loop is stable.

The simulation results show an intensity noise suppression of ∼50 dB and a slight increase in noise at higher frequencies. The simulations were carried out assuming a minimum pump power of 78 mW. Resetting the phase shift and the gain of the differentiator circuit in the feedback loop, this small (∼1 dB) increase in noise can be shifted to lower or higher frequencies according to the application requirements.

The Nyquist diagram of the simulated control loop is shown in Fig. 4. The instability point $(-1, 0)$ is not encompassed by the curve, so the loop is stable and has a maximum suppression at the relaxation oscillation frequency.

III. Optical Subsystem and Noise Characteristics

The crystal laser being used consists of a Nd:YVO_4 lasing material and a MgO:$LiNbO_3$ electrooptic material for the active mode-locking. Because of this mode-locking potential, this kind of crystal structure can be very useful in future millimeter-wave optical-wireless systems. The geometrical size of the microchip defines the frequency difference between the two active modes of the laser. In our case, these two modes are 20 GHz apart. Using a millimeter-wave oscillator for active mode locking at the electrooptic material, high-quality microwave generation is possible. This scheme is used for optical generation of microwaves in LMDS and optical-mobile networks [1], [2]. In order to be able to exploit this new way of optical generation and processing of microwaves, we have to eliminate the intensity noise peak of the laser.

In our setup used for noise suppression, the solid-state laser is optically pumped by an SCT100–808-Z1–01 high-power laser diode at 808 nm. The pump is temperature stabilized by a Peltier element and an LDT-5412 temperature controller. The laser diode has a maximum output power of 1.4 W at a current of 1.6 A.

The pump light is focused on the input mirror of the crystal by a Thorlabs C440TM-B (AR Coated 600–1050 nm) lens. When pumped by 1.2-W optical input power, the Nd:YVO_4 produces an output power of 200 mW. The 1064-nm output light is focused again by a C440TM-C (AR coated 1050–1550 nm) lens on a PT611 InGaAs photodiode. InGaAs PIN presents a major advantage over Si photodiodes. Using InGaAs receivers, the quantum noise can be neglected, which is generated by the attenuated portion of the 808-nm pump light. Because of the much

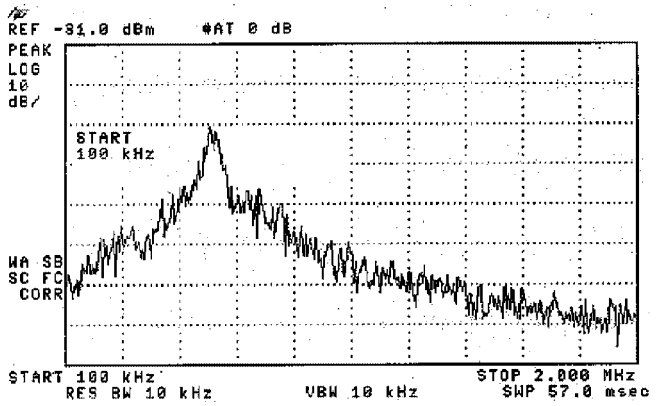

Fig. 5. The relative intensity noise peak of the Nd:YVO_4 crystal laser at a pump power of 100 mW (380 mA). The relaxation oscillation frequency is at 500 kHz. The measurement was taken by an HP8593E spectrum analyzer, under the following conditions. RES BW= 10 kHz, video BW= 10 kHz, no video averaging, Input attenuation = 0 dB.

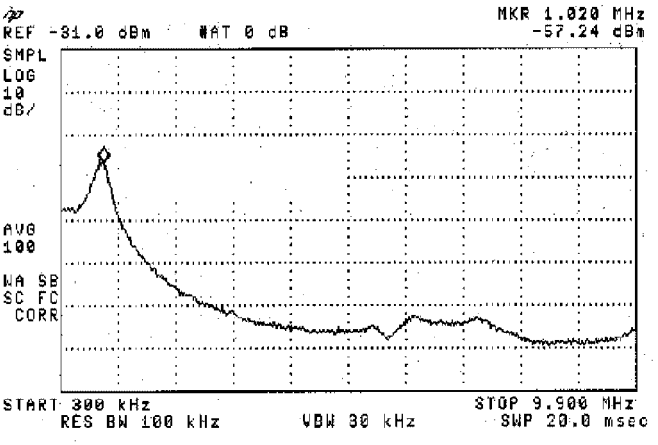

Fig. 6. Intensity noise at the relaxation frequency of 1020 kHz. The pump power was 350 mW (600-mA bias current across the laser diode). The measurement conditions are: Resolution BW= 100 kHz, video BW= 30 kHz, 100-point video averaging, Input attenuation = 0 dB.

less sensitivity of InGaAs at the pump wavelength and higher efficiency at 1064 nm, the RIN-to-quantum noise ratio increases. This special signal-to-noise ratio is a basic precondition for the proper operation of the feedback loop.

The relaxation oscillations peak appears at an offset frequency of 100 kHz–2 MHz on both of the laser modes (Fig. 1). The measured RIN peak is shown at different pump power in Figs. 5 and 6.

Figs. 5 and 6 show a 30–40 dB high pitch of noise at the relaxation resonance above the shot noise. The measured frequencies are congruent with the calculations. The signal was taken by an InGaAs photodiode followed by a 5-kΩ gain transimpedance amplifier. The detector was illuminated by a 10-mW fraction of the crystal output power. The maximum value of the noise curve was -50 dBm on the 50-Ω input impedance spectrum analyzer (Fig. 5). Taking into account the 5-kΩ transimpedance of the receiver, the 10-kHz resolution bandwidth of the spectrum analyzer (Fig. 5), and the $\eta = 0.8$ quantum efficiency of the InGaAs material at 1064 nm, a RIN value of -70 dBc/Hz can be evaluated. The slight difference caused by the Gaussian shape

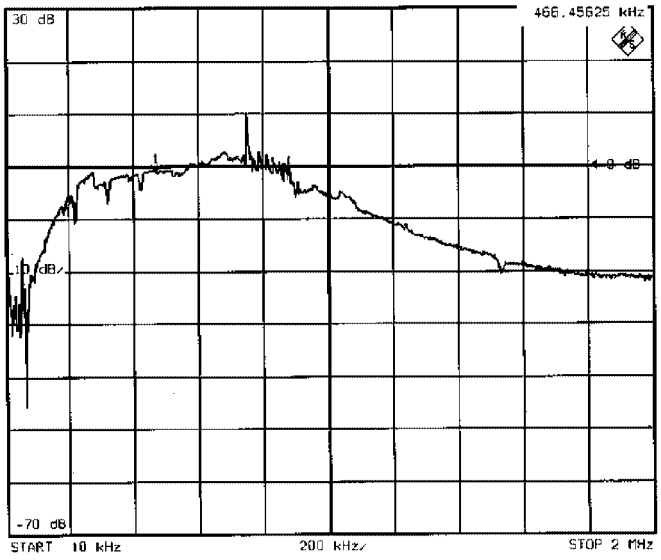

Fig. 7. The magnitude transfer function of the Nd:YVO_4 laser crystal at a pump power of 300 mW. The peak value is at 750 kHz. At these particular pump conditions, the laser transfer function is dominant over the measurement setup introduced noise floor, in the range of 100 kHz–1.5 MHz.

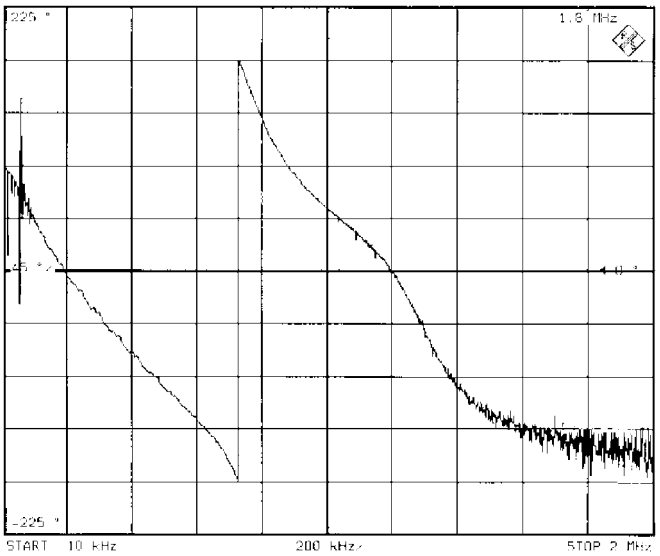

Fig. 8. The phase diagram of the laser transfer function. The pump power was 300 mW. The phase shift of the laser crystal is 180° at the relaxation oscillation. Above the transition frequency, the increasing phase shift of the diode driver circuit is domineering. (Span $=2$ MHz, input power$=-25$ dBm).

of the input filter in the spectrum analyzer was neglected during the calculation. This result characterizes the RIN performance of the Nd:YVO_4 laser at a pump power of 100 mW.

Fig. 6 shows the resonance at a pump power of 350 mW. In this case, the frequency span of the measurement setup was 10 MHz. As shown above, the influence of the intensity noise is decreasing above 2 MHz and the flat shot noise is getting dominant.

The difference between Figs. 5 and 6 shows that while raising the pump power, the frequency of the relaxation oscillations is also increasing. Similarly, the amplitude maximum of the resonance is also changing with the pump power. According to our measurements, a possible way of RIN reduction could be the use of higher pump power. The crystal laser being saturated, the amplitude of the relaxation resonance is decreasing. However, because of the danger of damaging the crystal and the quite small reduction of the noise peak, we have to apply an active optoelectronic control loop for noise suppression. Fig. 7 shows the magnitude transfer function of the Nd:YVO_4 laser rod, which delivers basic information for the feedback design. Fig. 8 presents the phase diagram of the crystal transfer function. The microchip laser has a phase shift of -180° at the frequency of the relaxation resonance. The further phase advance in the range above the resonance frequency is due to the phase shift of the laser diode driver circuit. Changing the pump power, the frequency of the 180° phase transition follows the frequency of the resonant peak. The transfer function was captured by a R&S 9 kHz–4 GHz vector network analyzer between the input of the pump laser diode driver circuit and the output of the photodiode. The results measured are in good agreement with the transfer model we have used during the simulations.

IV. Feedback Loop Electronics

The experimental arrangement of the electronics used for the intensity noise suppression can be seen in Fig. 9.

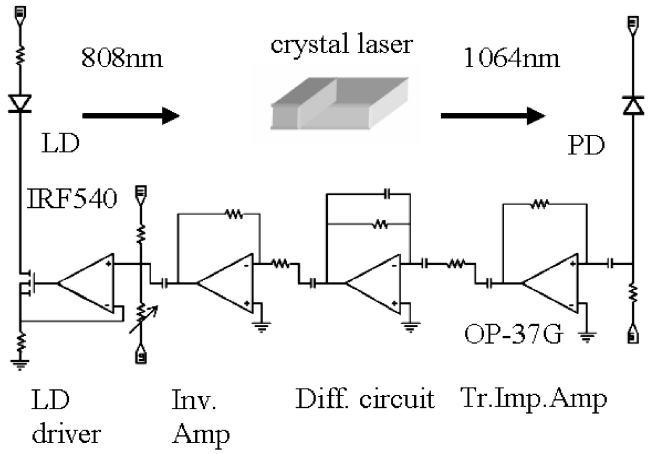

Fig. 9. Feedback loop electronics. The detected noise peak is amplified, differentiated, and added to the bias current of the pump laser diode.

A 10-mW fraction of the 1064-nm optical output power of the Nd:YVO_4 laser generated a dc photocurrent of 8 mA across the PT611–type InGaAs photodiode. The PIN was biased at -20 V. The transimpedance amplifier was built with a low-noise high-speed Analog Devices OP37G (voltage noise 3 nV $/\sqrt{\text{Hz}}$ max at 1 kHz, GBWP $=$ 63 MHz) type operational amplifier. The gain of the transimpedance amplifier was 5 kΩ. The next stage in the control loop was a differentiator circuit with a 6-dB/octave rising function of frequency in the range of 10 kHz–2 MHz and a phase shift of -90°. Because of the inverting run of the transimpedance amplifier and the differentiator circuit, an additional inverting amplifier circuit was necessary.

As a current supply for the laser diode, we have used an OP37G operational amplifier based voltage-to-current converter. In that circuit, an IRF540 low-cost power transistor delivers the 350 mA–1.6 A bias current. The current supply

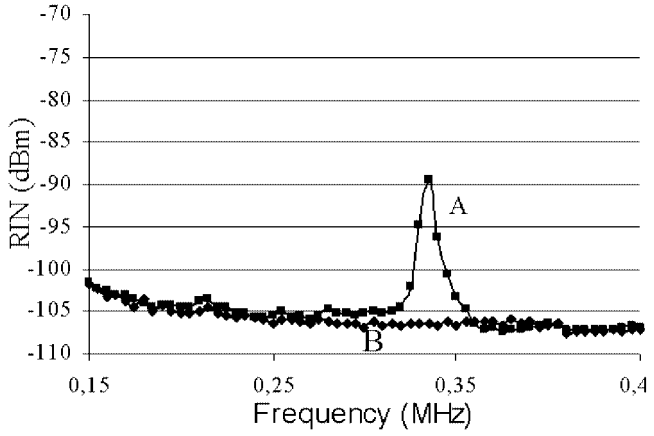

Fig. 10. The observed noise suppression at a pump power of 80 mW (300 mA). Curve A is the noise spectrum of the free-running laser; curve B presents the suppressed noise spectrum. The results were captured by an HP8593E spectrum analyzer and HP-VEE instrument control software. The measurement conditions were as follows: resolution BW $=$ 10 kHz, video BW $=$ 10 kHz, 100-point video averaging, input attenuation $=$ 0 dB.

defines a particular bias current throughout the laser diode and modulates the control signal onto the optical carrier.

V. Noise Suppression

The noise reduction achieved by feedbacking can be seen in Fig. 10.

The measured diagram shows an intensity noise suppression of 17 dB at the relaxation oscillation frequency. The difference of the measured suppression to the corresponding simulation results is due to the limited gain-bandwidth product of the OP37G operational amplifier. Increasing the amplifier gain in the feedback loop, the 50-dB suppression shown in the simulations is feasible. The suppression achieved can be further increased when reducing the overall noise level of the loop and thus enhance the RIN-to-noise ratio.

There is a slight increase of noise at frequencies above the resonance. This increment is at all frequencies within the unit radius circle around the $(-1, 0)$ point of the open-loop Nyquist diagram. Figs. 11 and 12 show the magnitude and phase of the laser crystal transfer function at a pump power of 80 mW, which was used at the noise reduction presented in Fig. 10. Similar to the case of the transfer measurements of Figs. 7 and 8, the frequency where the phase advance is -180° is the frequency of the relaxations oscillations too.

VI. Conclusion

In this paper, a system with capabilities suppressing the relative intensity noise peak of a Nd:YVO_4 microchip laser was demonstrated. During the system design, a simple model of the laser transfer function was applied. Using such a noise reduction circuit, the Nd:YVO_4 is a suitable choice for telecommunication applications because of its wide absorption spectrum, good phase noise characteristics, and mode-locking possibilities.

Additionally, noise investigations were carried out and the tuning of the resonance frequency was reported on.

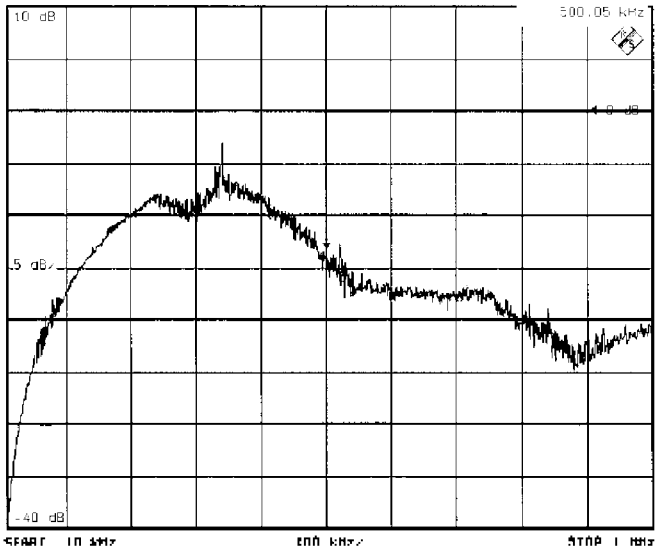

Fig. 11. Magnitude transfer function of the Nd:YVO_4 microchip laser at a pump power of 80 mW. Corresponding to the measured results in Fig. 10, the peak of the transfer function is located at 340 kHz. (Input power $=$ -25 dBm, span $=$ 1 MHz).

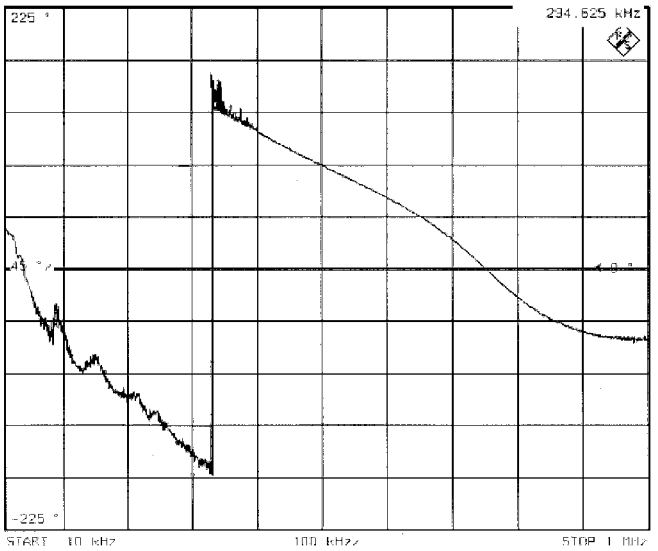

Fig. 12. Phase diagram of the microchip laser transfer function at a particular pump power of 80 mW. The measured suppression result at this pumping is depicted in Fig. 10. There is a 180° phase shift at the relaxation oscillations of 340 kHz. The measurement conditions are the same as in case of Fig. 11. Input power $=$ -25 dBm, span $=$ 1 MHz, no averaging.

References

[1] P. R. Herczfeld, "Overview of microwave photonics activity under MARC," in Optical/Wireless Workshop, Budapest, Hungary, Mar. 12, 2001G.

[2] W. D. Jemison, P. R. Herczfeld, W. Rosen, A. Vieira, A. Rosen, A. Paolella, and A. Joshi, "Hybrid fiberoptic-millimeter wave links," *IEEE Microwave Mag.*, vol. 1, June 2000.

[3] T. J. Kane, "Intensity noise in diode-pumped single-frequency Nd:YAG lasers and its control by electronic feedback," *IEEE Photon. Technol. Lett.*, vol. 2, Apr. 1990.

[4] C. C. Harb, M. B. Gray, H.-A. Bachor, R. Shilling, P. Rottengatter, I. Freitag, and H. Welling, "Suppression of the intensity noise in a diode-pumped neodymium:YAG nonlinear ring laser," *J. Quantum Electron.*, vol. 30, pp. 2907–2913, Dec. 1994.

[5] G. De Geronimo, S. Taccheo, and P. Laporta, "Optoelectronic feedback control for intensity noise suppression in a codoped erbium-ytterbium glass laser," *Electron. Lett.*, vol. 33, pp. 1336–1337, 1997.
[6] S. Taccheo, P. Laporta, O. Svelto, and G. De Geronimo, "Intensity noise reduction in a single-frequency ytterbium codoped erbium laser," *Opt. Lett.*, vol. 21, no. 21, pp. 1747–1749, Nov. 1996.
[7] T.-D. Ni, X. Zhang, and A. S. Daryoush, "Experimental study on close-in to microwave carrier phase noise of laser diode with external feedback," *IEEE Trans. Microwave Theory Tech.*, vol. 43, Sept. 1995.
[8] M. Csörnyei, T. Berceli, T. Bánky, T. Marozsák, and P. R. Herczfeld, "A new approach for RIN peak and phase noise suppression in microchip lasers," in *Int. Microwave Symp. (IMS2002)*, Seattle, WA, June 2–7, 2002, pp. 1377–80.
[9] W. Koechner, *Solid-State Laser Engineering*. Berlin/Heidelberg, Germany: Springer-Verlag, 1999.

Márk Csörnyei (S'03) was born in Budapest, Hungary, in 1977. He received the M.Sc. degree in electrical engineering from the Budapest University of Technology and Economics, Budapest, Hungary, in 2000 and is currently working toward the Ph.D. degree in electrical engineering at the same university.

His research interest include laser noise suppression and analysis of nonlinearities in fiber-radio systems.

Tibor Berceli (SM'77–F'94) was a Visiting Professor in the United States, United Kingdom, Germany, France, Finland, and Japan. He is a Professor of Electrical Engineering at the Budapest University of Technology and Economics, Budapest, Hungary. He instructs eight Ph.D. students, and he works on several European projects. He has published more than 170 papers in the field of microwave and optical communications, and he has written six books and invented 26 patents. His present research activity is in micowave photonics.

Peter R. Herczfeld (S'66–M'67–SM'89–F'91), photograph and biography not available at the time of publication.